ACS Medicinal Chemistry Letters

Letter

pubs.acs.org/acsmedchemlett

Structure-Based Design and Synthesis of Potent Cyclic Peptides Inhibiting the YAP–TEAD Protein–Protein Interaction

Zhisen Zhang,[†,‡] Zhaohu Lin,[†,§] Zheng Zhou,[†,§] Hong C. Shen,[†,‡] S. Frank Yan,[†,∥] Alexander V. Mayweg,[†,‡] Zhiheng Xu,[†,§] Ning Qin,[†,§] Jason C. Wong,[†,‡] Zhenshan Zhang,[†,∥] Yiping Rong,[†,⊥] David C. Fry,[#] and Taishan Hu*[,†,‡]

[†]Pharmaceutical Research and Early Development, [‡]Medicinal Chemistry, [§]Discovery Technology, [∥]Molecular Design and Chemical Biology, [⊥]Discovery Oncology, Roche Innovation Center Shanghai, Building 5, Lane 720, Cai Lun Road, Shanghai 201203, China

[#]Roche Research Center, Hoffmann-La Roche Inc., 340 Kingsland Street, Nutley, New Jersey 07110, United States

Supporting Information

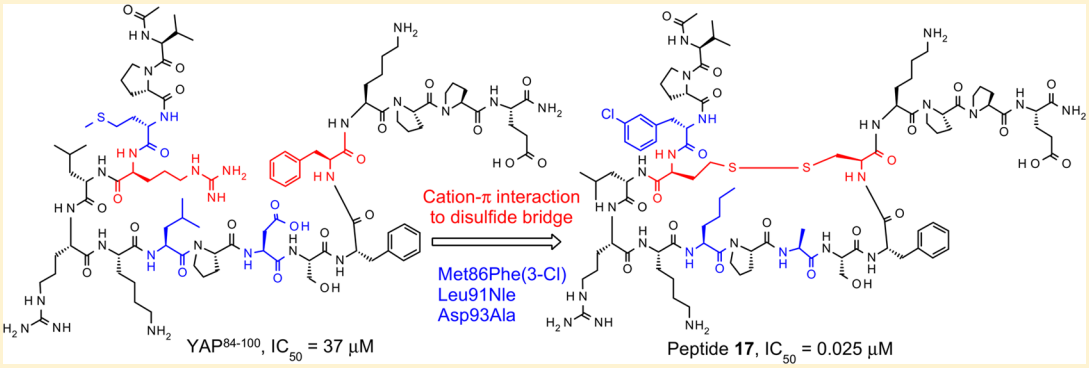

ABSTRACT: The YAP–TEAD protein–protein interaction (PPI) mediates the oncogenic function of YAP, and inhibitors of this PPI have potential usage in treatment of YAP-involved cancers. Here we report the design and synthesis of potent cyclic peptide inhibitors of the YAP–TEAD interaction. A truncation study of YAP interface 3 peptide identified YAP^{84-100} as a weak peptide inhibitor (IC_{50} = 37 μM), and an alanine scan revealed a beneficial mutation, D94A. Subsequent replacement of a native cation–π interaction with an optimized disulfide bridge for conformational constraint and synergistic effect between macrocyclization and modification at positions 91 and 93 greatly boosted inhibitory activity. Peptide **17** was identified with an IC_{50} of 25 nM, and the binding affinity (K_d = 15 nM) of this 17mer peptide to TEAD1 proved to be stronger than YAP^{50-171} (K_d = 40 nM).

KEYWORDS: *Peptide inhibitor, conformational constraint, YAP, TEAD, protein–protein interaction*

The Hippo signaling pathway plays an important role in organ size control by regulating cell proliferation and apoptosis.[1−3] Dysregulations of this pathway have been implicated in human tumorigenesis. Yes-associated protein (YAP) is the major downstream effector of the Hippo pathway, and not surprisingly, it functions as an oncogene. YAP gene is amplified in several human cancers,[4,5] and increased YAP expression and nuclear localization have been observed in liver cancers, colon cancers, ovarian cancers, lung cancers, and prostate cancers.[6−8] As a coactivator, YAP regulates gene transcription through its interaction with transcription factors. The TEA domain (TEAD) family was found to play a key role in mediating the growth-promoting function of YAP.[9,10] Knockdown of TEADs or disruption of YAP–TEAD interaction diminished the majority of YAP-dependent gene expression and YAP functions in promoting cell proliferation, oncogenic transformation, and epithelial–mesenchymal transition (EMT). In addition, the phenotype of TEAD1/TEAD2 double-knockout mice resembled YAP knockout mice with decreased proliferation and increased apoptosis.[11] Very recently, it was reported that verteporfin was able to interrupt YAP–TEAD interaction by binding to YAP and suppressed liver overgrowth caused by YAP overexpression or activation[12] and human retinoblastoma cell growth.[13] All these results suggest that blocking YAP–TEAD interaction can abolish the oncogenic function of YAP, and inhibitors of YAP–TEAD interaction could have potential therapeutic use for treatment of cancers where YAP is overexpressed or activated.

Historically, protein–protein interactions (PPIs) have been considered undruggable due to their much larger interaction surface areas and less well-defined shape than conventional substrate-binding cavities. However, with the increasing understanding of the nature of PPIs, emerging drug discovery

Received: April 24, 2014
Accepted: July 13, 2014
Published: July 14, 2014

   dx.doi.org/10.1021/ml500160m | ACS Med. Chem. Lett. 2014, 5, 993−998

technology, and recent successful cases,[14−17] PPIs have become more feasible drug targets. The YAP−TEAD PPI is mediated by YAP's TEAD-binding domain (TBD) and TEAD's YAP-binding domain (YBD). Located at the N terminus, YAP TBD is natively unfolded, while TEAD YBD is at the C-terminal region adopting a globular structure.[18] The crystal structure of the human YAP−TEAD complex reveals that YAP TBD becomes highly structured after being bound, and it wraps around TEAD via three interfaces (Figure 1).[19] The third

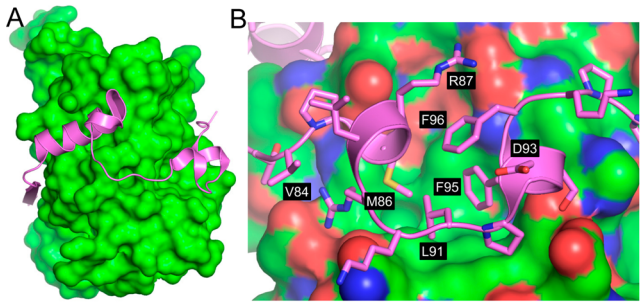

Figure 1. YAP−TEAD complex (PDB code: 3KYS). (A) TEAD is depicted as a surface representation in green, and YAP as a cartoon in violet with 3 interfaces, a β strand, an α helix, and a twist coil shown. (B) A zoomed-in view of interface 3. The surface of TEAD is colored by atoms (carbon in green, oxygen in red, and nitrogen in blue). YAP is in violet cartoon representation, and residues are in sticks colored with carbon in violet, oxygen in red, nitrogen in blue, and sulfur in yellow.

interface, YAP^{86-100} (residues 86−100), is a twisted-coil fitting into a hydrophobic pocket on the surface of TEAD and was reported to be most important to the YAP−TEAD interaction. Since the use of an interface peptide represents a valid approach to identify PPI inhibitors, we sought to optimize this YAP peptide by conformational constraint and key residue modification in order to identify potential biological tools and prototype therapeutics. Herein we report the design and synthesis of potent cyclic peptide inhibitors targeting the YAP−TEAD PPI.

The study commenced with YAP^{81-100} peptide (^{81}PQTVPMRLRKLPDSFFKPPE^{100}) instead of YAP^{86-100}, given that ^{81}PQTVP^{85}, a part of a loop located at the N terminus of YAP^{86-100}, was reported essential for YAP's binding to TEAD and for Yki to Sd (homologues of YAP and TEAD, respectively, in *Drosophila*).[20,21] Using a competitive binding assay based on surface plasmon resonance (SPR) to test the ability of peptides to disrupt the (His-YAP^{50-171})−(GST-$TEAD1^{209-426}$) complex, terminal truncation and alanine scan studies were conducted to identify the minimal active sequence and key amino-acid residues (Table 1).[22] Parent peptide YAP^{81-100} showed weak inhibitory activity with IC_{50} around 49 μM. Truncation study revealed that three N-terminal residues (PQT) were dispensable, and marginal activity improvement was actually observed with their deletion (YAP^{84-100} vs YAP^{81-100}). Further truncation of Val84 (YAP^{85-100}) and Pro85 (YAP^{86-100}) decreased the activity substantially, and as high as a 100-fold loss of activity was observed (peptides **S26** vs **8**, Table S5, Supporting Information). Val84 is engaged in an intramolecular hydrogen bond between its backbone carbonyl and the guanidinium NH of Arg87. Furthermore, the fact that V84A mutation (Table 1, YAP^{V84A}) could not maintain activity suggests that V84 provides a steric shielding effect on protein/peptide folding. This effect may also be invoked to explain the importance of Pro85. At the C-terminus, deletion of Glu100 (YAP^{81-99}) had little effect (See also peptides **S27** vs **8**, Table S5, Supporting Information), while the removal of Pro99 (YAP^{81-98}) and Pro98 (YAP^{81-97}) did harm the activity (see also peptides **S29** vs **S27**, Table S5, Supporting Information). However, alanine scan (Table 1, from YAP^{T83A} to YAP^{E100A}) illustrated the importance of each individual residue. The well-documented key residues,[19] Met86, Arg89 (forming a hydrogen bond with Asp264 of TEAD1, see Supporting Information), Leu91, Ser94 (forming hydrogen bonds with Tyr421 and Glu255 of TEAD1, respectively), Phe95, and Phe96 were confirmed here, as alanine substitution at each of these residues led to a complete loss of activity. In addition, Pro92 was found to be another essential residue. Apparently, residues Val84, Pro85, and Arg87 were more important than Thr83, Leu88, Lys90, Lys97, Pro98, and Pro99. E100A mutation maintained the activity (YAP^{E100A} vs YAP^{81-100}), which, together with truncation study (*vide supra*), indicated that Glu100 did not contribute to the YAP−TEAD interaction. In contrast to mutations at other positions, a 2-fold activity improvement was realized for D93A, which is presumably due to the α helix stabilization nature of alanine, considering the existence of a one-turn helix in that region (Figure 1B). Another piece of information supporting this assumption is that a more profound activity improvement could be achieved by Aib (2-aminoisobutyric acid) substitution at this position (Table S1, Supporting Information). A D-amino acid scan was also performed, providing similar results to the alanine scan (Figure S4, Supporting Information). Therefore, YAP^{84-99} was concluded to be the shortest peptide with meaningful inhibitory activity against YAP−TEAD PPI, and an overall picture of the importance of each amino acid residue to the YAP−TEAD interaction was obtained.

The cocrystal structure of the YAP−TEAD complex revealed that Arg87 and Phe96 in YAP are spatially close (Figure 1B and PDB 3KYS). The distance between the guanidinium carbon of Arg and the aromatic center of Phe is less than 5 Å, indicating a cation−π interaction between the two residues.[23] Since these two residues were not involved in direct interaction with TEAD, we speculated that this cation−π interaction could be replaced by a more robust covalent bond via the macrocyclization strategy, which could lead to a much better global conformational constraint effect,[22] thereby conferring better activity as well as plasma stability. Given that the two residues are located in the middle of the peptide, side chain to side chain cyclization was envisioned. Various lactam bridges were tested first. However, the resulting cyclic peptides were totally inactive (data not shown). We then turned our attention to disulfide bridges, a strategy widely used by nature for protein conformational constraint. Two thio-containing amino acids, cysteine and homocysteine (Hcy), were explored as substituents at positions 87 and 96 (Table 2, peptides **1**−**5**), respectively. Remarkably, peptide **3** with a disulfide bond formed from Hcy87 and Cys96 was found to be 5-fold more potent than the parent YAP^{84-100}. Substitutions the other way around (peptide **2**), that is, Cys87 and Hcy96, were not as potent, and the resulting peptide was 14 times less active than peptide **3**. Interestingly, disulfide peptide **1** with Cys87 and Cys96 and disulfide peptide **4** with Hcy87 and Hcy96 were not active at all, though they are just one CH_2 (methylene unit) different in ring size from peptide **3**. Apparently, both ring size and the exact location of the disulfide bond within the

dx.doi.org/10.1021/ml500160m | ACS Med. Chem. Lett. 2014, 5, 993−998

Table 1. N- and C-Terminal Truncation and Alanine Scan of YAP$^{81\text{-}100}$

peptide[a]	sequence	% inhib @ 50 μM[b]	IC_{50} (μM)[c]
YAP$^{81-100}$	PQTVPMRLRKLPDSFFKPPE	60	49
YAP$^{82-100}$	QTVPMRLRKLPDSFFKPPE	59	
YAP$^{83-100}$	TVPMRLRKLPDSFFKPPE	60	
YAP$^{84-100}$	VPMRLRKLPDSFFKPPE	62	37
YAP$^{85-100}$	PMRLRKLPDSFFKPPE	25	
YAP$^{86-100}$	MRLRKLPDSFFKPPE	12	
YAP$^{87-100}$	RLRKLPDSFFKPPE	12	
YAP$^{81-99}$	PQTVPMRLRKLPDSFFKPP	52	
YAP$^{81-98}$	PQTVPMRLRKLPDSFFKP	42	
YAP$^{81-97}$	PQTVPMRLRKLPDSFFK	14	
YAP$^{81-96}$	PQTVPMRLRKLPDSFF	13	
YAP$^{81-95}$	PQTVPMRLRKLPDSF	5.4	
YAP^{T83A}	PQ**A**VPMRLRKLPDSFFKPPE	52	
YAP^{V84A}	PQT**A**PMRLRKLPDSFFKPPE	26	
YAP^{P85A}	PQTV**A**MRLRKLPDSFFKPPE	33	
YAP^{M86A}	PQTVP**A**RLRKLPDSFFKPPE	1.3	
YAP^{R87A}	PQTVPM**A**LRKLPDSFFKPPE	23	
YAP^{L88A}	PQTVPMR**A**RKLPDSFFKPPE	49	
YAP^{R89A}	PQTVPMRL**A**KLPDSFFKPPE	1.7	
YAP^{K90A}	PQTVPMRLR**A**LPDSFFKPPE	42	
YAP^{L91A}	PQTVPMRLRK**A**PDSFFKPPE	0.0	
YAP^{P92A}	PQTVPMRLRKL**A**DSFFKPPE	0.0	
YAP^{D93A}	PQTVPMRLRKLP**A**SFFKPPE	83	25
YAP^{S94A}	PQTVPMRLRKLPD**A**FFKPPE	1.6	
YAP^{F95A}	PQTVPMRLRKLPDS**A**FKPPE	4.0	
YAP^{F96A}	PQTVPMRLRKLPDSF**A**KPPE	9.4	
YAP^{K97A}	PQTVPMRLRKLPDSFF**A**PPE	42	
YAP^{P98A}	PQTVPMRLRKLPDSFFK**A**PE	47	
YAP^{P99A}	PQTVPMRLRKLPDSFFKP**A**E	41	
YAP^{E100A}	PQTVPMRLRKLPDSFFKPP**A**	71	43

[a]Synthetic peptides in this letter are N-terminal acetylated and C-terminal amidated unless otherwise indicated. [b]Percentage inhibition at concentration of 50 μM. [c]Half maximal inhibitory concentration; blank spaces denote not determined.

macrocyclic linkage are critical for mimicking the cation−π interaction. Conversely, peptide **5**, the corresponding open-chain counterpart of **3**, did not show any activity, illustrating the importance of conformational constraint by cyclization. The D93A mutation was also found beneficial in the context of the cyclic peptide, and peptide **6** was 4-fold more active than peptide **3**.

After successfully identifying a disulfide as an excellent surrogate of the cation−π interaction between Arg87 and Phe96, we continued to improve peptide activity by key residue modification. Met86, Leu91, and Phe95, which are involved in hydrophobic interactions with TEAD, stood out as the preferred sites for modification. Starting from residue Leu91 (Table 2, peptides **7**−**12**; see also Table S2 in Supporting Information), we first replaced it with its straight side chain homologue, norleucine (Nle), which resulted in a 4-fold activity increase (peptides **7** vs **3**). The D93A mutation was then executed here again. Surprisingly, this maneuver rendered a 10-fold activity boost from peptide **7** to peptide **8** with an IC_{50} of 0.15 μM. Comparing the extent of improvement caused by the D93A mutation in a different context (*vide supra*), we conclude that there is a synergistic effect between D93A, L91Nle, and macrocyclization, which led to a 250-fold total activity improvement (peptide **8** vs YAP$^{84-100}$). Elongation by one CH_2 at the side chain of Nle provided further activity improvement, leading to peptide **9** with an IC_{50} of 0.04 μM. However, further side chain elongation (peptide **10**) was detrimental, as were branched side chains (peptides **11** and **12**). Next we modified Met86 (peptides **13**−**18**), while keeping Nle at position 91 due to its better availability than (*S*)-2-amino-heptanoic acid (Ahe) though the latter fit better here (peptides **9** vs **8**). Nle, as an isosteric analogue of methionine, did not function as well as Met (peptides **13** vs **8**). However, extension of the side chain with one CH_2 greatly improved the activity to 0.04 μM (peptide **14**). Aromatic side chains were also studied. *meta*-Chloro substituted phenylalanine (Phe(3-Cl)) demonstrated by far the best activity with an IC_{50} of 0.025 μM (peptide **17**), while *ortho*- and *para*-chlorinated phenylalanines (peptides **16** and **18**, respectively) as well as phenylalanine itself (peptide **15**) decreased the activity (vs **8**) and were >15-fold less potent than the corresponding meta-substituted analogue. Compared to positions 86 and 91, there seemed to be less tolerance at position 95 for modification (Table S4, Supporting Information), and *para*-fluorinated phenylalanine (Phe(4-F)) proved to be the best residue (Table 2, peptide **19**). Though 3-chlorophenylalanine, (*S*)-2-amino-heptanoic acid, and 4-fluorophenylalanine were the optimal residues at positions 86, 91, and 95, respectively, combination of these residues did not yield peptides superior to peptide **17** (Table S4, Supporting Information). This could be due to the fact that these 3 residues reside in the same hydrophobic pocket (Figure 1B) and may interfere with each other.

In order to rationalize the potency difference of the various peptides, we carried out computer modeling to investigate the

dx.doi.org/10.1021/ml500160m | ACS Med. Chem. Lett. 2014, 5, 993−998

Table 2. Replacement of Cation–π Interaction between Positions 87 and 96 with Disulfide Bridge, and Modification at Positions 86, 91, and 95 in YAP$^{84\text{-}100}$

peptide	annotation	sequence[a]																IC_{50} (μM)
1	cyclo-[Cys^{87}-Cys^{96}]	V	P^{85}	Met	Cys	L	R	K^{90}	Leu	P	D	S	Phe^{95}	Cys	K	P	P	E^{100}	>100
2	cyclo-[Cys^{87}-Hcy^{96}]	V	P	Met	Cys	L	R	K	Leu	P	D	S	Phe	Hcy	K	P	P	E	85
3	cyclo-[Hcy^{87}-Cys^{96}]	V	P	Met	Hcy	L	R	K	Leu	P	D	S	Phe	Cys	K	P	P	E	6.9
4	cyclo-[Hcy^{87}-Hcy^{96}]	V	P	Met	Hcy	L	R	K	Leu	P	D	S	Phe	Hcy	K	P	P	E	>100
5	Open chain	V	P	Met	Hcy	L	R	K	Leu	P	D	S	Phe	Cys	K	P	P	E	>100
6	cyclo-[Hcy^{87}-Cys^{96}]	V	P	Met	Hcy	L	R	K	Leu	P	A	S	Phe	Cys	K	P	P	E	1.5
7	cyclo-[Hcy^{87}-Cys^{96}]	V	P	Met	Hcy	L	R	K	Nle	P	D	S	Phe	Cys	K	P	P	E	1.7
8	cyclo-[Hcy^{87}-Cys^{96}]	V	P	Met	Hcy	L	R	K	Nle	P	A	S	Phe	Cys	K	P	P	E	0.15
9	cyclo-[Hcy^{87}-Cys^{96}]	V	P	Met	Hcy	L	R	K	Ahe	P	A	S	Phe	Cys	K	P	P	E	0.042
10	cyclo-[Hcy^{87}-Cys^{96}]	V	P	Met	Hcy	L	R	K	Aoc	P	A	S	Phe	Cys	K	P	P	E	0.37
11	cyclo-[Hcy^{87}-Cys^{96}]	V	P	Met	Hcy	L	R	K	Hle	P	A	S	Phe	Cys	K	P	P	E	0.62
12	cyclo-[Hcy^{87}-Cys^{96}]	V	P	Met	Hcy	L	R	K	Amh	P	A	S	Phe	Cys	K	P	P	E	0.31
13	cyclo-[Hcy^{87}-Cys^{96}]	V	P	Nle	Hcy	L	R	K	Nle	P	A	S	Phe	Cys	K	P	P	E	0.34
14	cyclo-[Hcy^{87}-Cys^{96}]	V	P	Ahe	Hcy	L	R	K	Nle	P	A	S	Phe	Cys	K	P	P	E	0.041
15	cyclo-[Hcy^{87}-Cys^{96}]	V	P	Phe	Hcy	L	R	K	Nle	P	A	S	Phe	Cys	K	P	P	E	0.35
16	cyclo-[Hcy^{87}-Cys^{96}]	V	P	Phe(2-Cl)	Hcy	L	R	K	Nle	P	A	S	Phe	Cys	K	P	P	E	0.38
17	cyclo-[Hcy^{87}-Cys^{96}]	V	P	Phe(3-Cl)	Hcy	L	R	K	Nle	P	A	S	Phe	Cys	K	P	P	E	0.025
18	cyclo-[Hcy^{87}-Cys^{96}]	V	P	Phe(4-Cl)	Hcy	L	R	K	Nle	P	A	S	Phe	Cys	K	P	P	E	0.53
19	cyclo-[Hcy^{87}-Cys^{96}]	V	P	Met	Hcy	L	R	K	Nle	P	A	S	Phe(4-F)	Cys	K	P	P	E	0.075

[a]Abbreviation for some special amino acids: Hcy, homocysteine; Nle, norleucine; Ahe, (*S*)-2-amino-heptanoic acid; Aoc, (*S*)-2-amino-octanoic acid; Hle, L-homoleucine; Amh, (*S*)-2-amino-6-methyl-heptanoic acid.

dx.doi.org/10.1021/ml500160m | ACS Med. Chem. Lett. 2014, 5, 993−998

interaction between the cyclic peptide and TEAD protein on a molecular level. The difference observed from modification at position 86, especially for chlorophenylalanines, could be explained rationally (Figure 2). As illustrated in Figure 2A, the

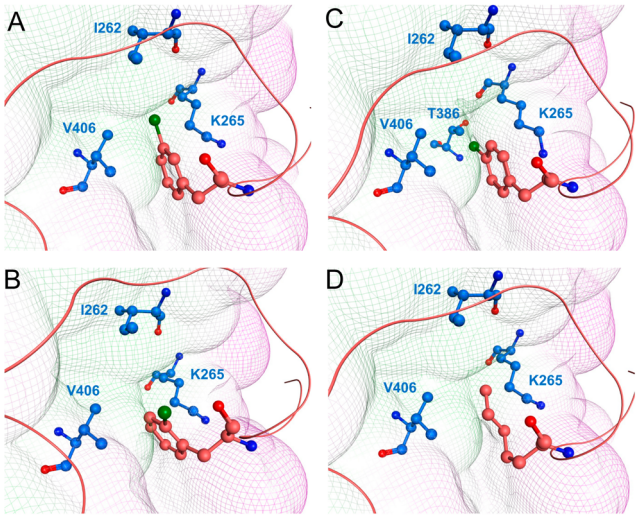

Figure 2. Interactions of peptides **17** (A), **16** (B), **18** (C), and **14** (D) with TEAD1, respectively, by computer modeling. The van der Waals interaction surface between TEAD1 and peptide is represented as line surface colored with lipophilic interaction in green, neutral in white, and hydrophilic in magenta. The TEAD1 residues I262, K265, V406, and T386 are highlighted in ball and stick representation with carbon in blue. Peptides are represented as a ribbon in light red, and only residues at position 86 are shown in ball and stick for clarity with carbon in light red. The nitrogen atom is always colored in blue, oxygen in red, and chlorine in dark green.

meta-Cl-phenyl ring of Phe(3-Cl) in peptide **17** forms extensive hydrophobic interactions with Val406, Ile262, and the side chain of Lys265 of TEAD1. Furthermore, the chlorine atom and the phenyl ring contact perfectly with the van der Waals interaction surface of TEAD1, indicating favorable van der Waals interaction with the protein. In contrast, the chlorine atom of Phe(2-Cl) in peptide **16** is largely solvent exposed without much interaction with the protein (Figure 2B), consistent with the similar activity between peptides **16** and **15**. In the case of peptide **18**, the chlorine atom of Phe(4-Cl) would protrude into the TEAD1 interaction surface and cause mild clashes with Lys265, Val4061, and Thr386, which consequently resulted in a certain level of distortion in the TEAD1 protein and rearrangements particularly of the interfacing residues (Figure 2C), in line with the much decreased activity. Figure 2D depicts the interaction between peptide **14** and TEAD1. The side chain of Ahe86 in peptide **14** undergoes a favorable hydrophobic interaction with TEAD1 with its orientation apparently similar to Phe(3-Cl) in peptide **17**, rendering its good activity.

To gain more insight into conformational changes of the peptide after macrocyclization, a ^{1}H NMR study of peptide **8** was performed. The data in d^{6}-DMSO indeed showed peptide **8** produced nuclear Overhauser effects (NOEs), but no evidence indicated that it was locked into one unique conformation. Therefore, the peptide was somewhat flexible but not completely floppy. Pro92, the newly identified key residue, existed in two conformers in a *trans*/*cis* ratio of 3.5:1. There was a large NOE in the minor species between the Cα-H of Nle91 and that of Pro92, diagnostic of a *cis* conformation at this peptide bond (Figure S6, Supporting Information). In addition, the minor Pro92 Cα-H (4.48 ppm) moved downfield with respect to where it was for the major species (4.23 ppm), also consistent with the conversion to *cis*. The exchange between the two conformers was quite slow. The other three prolines, Pro85, Pro98, and Pro99, appeared to be essentially all *trans*. Co-crystallization of our peptides with TEAD was also attempted, yet without success. Fortunately, we were able to coexpress [Cys^{87}, Ala^{93}, Cys^{96}, Arg^{100}]-YAP$^{50-171}$ and TEAD1$^{209-426}$ in an *E. coli* system, and successfully solved their cocrystal structure. The secondary structure of this quadruple YAP mutant was well retained with the core root-mean-square deviation (rmsd) as 0.81 Å when superimposed to the wild-type YAP structure (PDB: 3KYS). A disulfide bond between Cys^{87} and Cys^{96} was unambiguously determined, which indicated the critical contribution of the disulfide bridge to rigidifying the YAP conformation and to the PPI interaction.[24]

We further evaluated the competitive activity of some representative peptides against endogenous YAP binding to GST-TEAD1$^{209-426}$ in a GST pull-down assay (Figure 3A). As

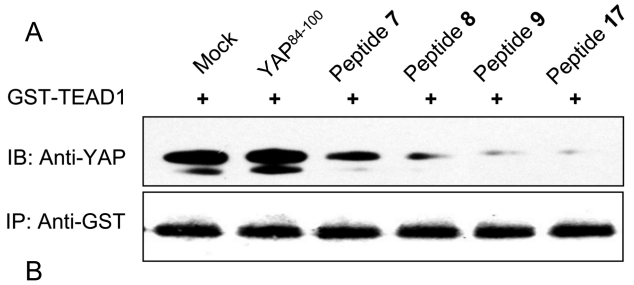

B

Peptide	7	8	9	17	His-YAP$^{50-171}$
K_d (nM)	211	39	18	15	40

Figure 3. (A) GST pull-down assay. Peptides competed with endogenous YAP protein binding to GST-TEAD1$^{209-426}$ in a pull-down assay with 20 μL of glutathione sepharose beads, 5 μg of GST-TEAD1$^{209-426}$, Bel-7404 human hepatoma cell lysate (0.2 mg), and peptides (2 μM) in 1 mL of lysis buffer. Binding proteins were analyzed by SDS-PAGE and Western blotting. See Supporting Information for experimental details. (B) Binding affinity (K_d) of peptides and His-YAP$^{50-171}$ to GST-TEAD1$^{209-426}$.

can be seen, the wild-type peptide YAP$^{84-100}$ did not work, while all 4 disulfides tested showed substantial inhibitory activity with peptides **9** and **17** being the most potent ones. The binding affinity of the 4 disulfides to GST-TEAD1$^{209-426}$ was also measured by Biacore (Figure 3B). Consistent with the pull-down assay, peptides **9** and **17** showed the strongest binding affinity with dissociation constants (K_d) of 18 and 15 nM, respectively. As a benchmark, the K_d of His-YAP$^{50-171}$ was determined to be 40 nM, which is close to that of YAP$^{2-268}$ to TEAD2$^{217-447}$ (33 nM) measured by isothermal titration calorimetry.[18]

Cell permeability and plasma stability are two often faced challenges in peptide drug discovery. Conjugation of our cyclic peptide at the C-terminal with cell penetrating peptide like TAT enabled cell penetrating; however, it also led to some level of cell membrane damage (data not shown). Apparently

dx.doi.org/10.1021/ml500160m | ACS Med. Chem. Lett. 2014, 5, 993−998

alternative intracellular delivery technologies may be needed. However, cyclization marginally improved plasma stability, and incorporation of K90k mutation could dramatically increase a peptide's resistance to proteolytic degradation (Table S6, Supporting Information).

In conclusion, a disulfide bridge was successfully employed as a surrogate for a cation−π interaction for peptide conformational constraint, and potent 17mer peptide inhibitors against YAP−TEAD PPI were identified. In particular, synthetic peptides such as **17** demonstrated stronger binding affinity to TEAD1 than the YAP protein. Substantial structure−activity relationship (SAR) information on interface 3 of the PPI was obtained. The binding affinity of YAP to TEAD could be significantly enhanced by improving the hydrophobicity at residues Met86, Leu91, and Phe95 of YAP, yet to capture hydrogen bonds like between Ser92 of YAP and Tyr421 and Glu255 of TEAD is important. Residue K90 is a potential place for further improvement both in potency and plasma stability. All this information should be very useful in the search for peptidomimetic and small molecule inhibitors of the YAP−TEAD interaction.[25]

■ ASSOCIATED CONTENT

Supporting Information

Experimental procedures, additional data on modification at positions 86, 91, and 95, truncation study of peptide **8**, plasma stability, ^{1}H NMR and NOESY of peptide **8**, and mass data. Numbering of TEAD1 in this paper follows UniProtKB/Swiss-Prot: P28347.2. This material is available free of charge via the Internet at http://pubs.acs.org.

■ AUTHOR INFORMATION

Corresponding Author

*(T.H.) E-mail: taishan.hu@roche.com.

Notes

The authors declare no competing financial interest.

■ REFERENCES

(1) Zhao, B.; Lei, Q.; Guan, K.-L. The Hippo-YAP pathway in organ size control and tumorigenesis: an updated version. *Genes Dev.* **2010**, *24*, 862−847.

(2) Harvey, K. F.; Zhang, X.; Thomas, D. M. The Hippo pathway and human cancer. *Nat. Rev. Cancer* **2013**, *13*, 246−257.

(3) Liu, A. M.; Xue, M. Z.; Chen, J.; Poon, R. T.; Luk, J. M. Targeting YAP and Hippo signalling pathway in liver cancer. *Expert Opin. Ther. Targets* **2010**, *14*, 855−874.

(4) Baldwin, C.; Garnis, C.; Zhang, L.; Rosin, M. P.; Lam, W. L. Multiple microalterations detected at high frequency in oral cancer. *Cancer Res.* **2005**, *65*, 7561−7567.

(5) Fernandez, L. A.; Northcott, P. A.; Dalton, J.; Fraga, C.; Ellison, D.; Angers, S.; Taylor, M. D.; Kenney, A. M. YAP1 is amplified and up-regulated in hedgehog-associated medulloblastomas and mediates Sonic hedgehog-driven neural precursor proliferation. *Genes Dev.* **2009**, *23*, 2729−2741.

(6) Zender, L.; Spector, M. S.; Xue, W.; Flemming, P.; Cordon-Cardo, C.; Silke, J.; Fan, S. T.; Luk, J. M.; Wigler, M.; Hannon, G. J.; Mu, D.; Lucito, R.; Powers, S.; Lowe, S. W. Identification and validation of oncogenes in liver cancer suing an integrative oncogenomic approach. *Cell* **2006**, *125*, 1253−1267.

(7) Zhao, B.; Wei, X.; Li, W.; Udan, R. S.; Yang, Q.; Kim, J.; Xie, J.; Ikenoue, T.; Yu, J.; Li, L.; Zheng, P.; Ye, K.; Chinnaiyan, A.; Halder, G.; Lai, Z. C.; Guan, K. L. Inactivation of YAP oncoprotein by the Hippo pathway is involved in cell contact inhibition and tissue growth control. *Genes Dev.* **2007**, *21*, 2747−2761.

(8) Steinhardt, A. A.; Gayyed, M. F.; Klein, A. P.; Dong, J.; Maitra, A.; Pan, D.; Montgomery, E. A.; Anders, R. A. Expression of Yes-associated protein in common solid tumors. *Hum. Pathol.* **2008**, *39*, 1582−1589.

(9) Zhao, B.; Ye, X.; Xu, J.; Li, L.; Li, W.; Li, S.; Lin, J. D.; Wang, C. Y.; Chinnaiyan, A. M.; Lai, Z. C.; et al. TEAD mediates YAP-dependent gene induction and growth control. *Genes Dev.* **2008**, *22*, 1962−1971.

(10) Ota, M.; Sasaki, H. Mammalian Tead proteins regulate cell proliferation and contact inhibition as transcriptional mediators of Hippo signalling. *Development* **2008**, *135*, 4059−4069.

(11) Sawada, A.; Kiyonari, H.; Ukita, K.; Nishioka, N.; Imuta, Y.; Sasaki, H. Redundant roles of Tead1 and Tead2 in notochord development and the regulation of cell proliferation and survival. *Mol. Cell. Biol.* **2008**, *28*, 3177−3189.

(12) Liu-Chittenden, Y.; Huang, B.; Shim, J. S.; Chen, Q.; Lee, S.-J.; Anders, R. A.; Liu, J. O.; Pan, D. Genetic and pharmacological disruption of the TEAD-YAP complex suppressed the oncogenic activity of YAP. *Genes Dev.* **2012**, *26*, 1300−1305.

(13) Brodowska, K.; Al-Moujahed, A.; Marmalidou, A.; Horste, M. M. Z.; Cichy, J.; Miller, J. W.; Gragoudas, E.; Vavvas, D. G. The clinically used phtosensitizer Verteporfin (VP) inhibits YAP−TEAD and human retinoblastoma cell growth in vitro without light activation. *Exp. Eye Res.* **2014**, *124*, 67−73.

(14) Fry, D. C. Protein-protein interactions as targets for small molecule drug discovery. *Biopolymers* **2006**, *84*, 535−552.

(15) Vega, M. P. D.; Martin-Martinez, M.; Gonzalez-Muniz, R. Modulation of protein-protein interactions by stabilization/mimicking protein secondary structure elements. *Curr. Top. Med. Chem.* **2007**, *7*, 33−62.

(16) Keskin, O.; Gursoy, A.; Ma, B.; Nussinov, R. Principles of protein-protein interactions: what are the preferred ways for proteins to interact? *Chem. Rev.* **2008**, *108*, 1225−1244.

(17) Azzarito, V.; Long, K.; Murphy, N.; Wilson, A. Inhibition of α-helix-mediated protein-protein interactions using designed molecules. *Nat. Chem.* **2013**, *5*, 161−173.

(18) Tian, W.; Wu, J.; Tomchick, D. R.; Pan, D.; Luo, X. Structural and functional analysis of the YAP-binding domain of human TEAD2. *Proc. Natl. Acad. Sci. U.S.A.* **2010**, *107*, 7293−7298.

(19) Li, Z.; Zhao, B.; Wang, P.; Chen, F.; Dong, Z.; Yang, H.; Guang, K.-L.; Xu, Y. Structural insights into the YAP and TEAD complex. *Genes Dev.* **2010**, *24*, 235−240.

(20) Chen, Li.; Chan, S. W.; Zhang, X.; Walsh, M.; Lim, C. J.; Hong, W.; Song, H. Structural basis of YAP recognition by TEAD4 in the Hippo pathway. *Genes Dev.* **2010**, *24*, 290−300.

(21) Wu, S.; Liu, Y.; Zheng, Y.; Dong, J.; Pan, D. The TEAD/TEF family protein scalloped mediates transcriptional output of Hippo growth-regulatory pathway. *Dev. Cell* **2008**, *14*, 388−398.

(22) Hruby, V. J. Designing peptide receptor agonists and antagonists. *Nat. Rev. Drug Discovery* **2002**, *1*, 847−858.

(23) Gallivan, J. P.; Dougherty, D. A. Cation-π interactions in structural biology. *Proc. Natl. Acad. Sci. U.S.A.* **1999**, *96*, 9459−9464.

(24) The detailed discussion of the cocrystal structure will be reported elsewhere.

(25) After completion of this manuscript, a hybrid peptide derived from hYAP$^{74-100}$ and hVGLL4$^{236-252}$ was reported to be able to suppress tumor growth in gastric cancer mouse models. Jiao, S.; Wang, H.; Shi, Z.; Dong, A.; Zhang, W.; Song, X.; He, F.; Wang, Y.; Zhang, Z.; Wang, W.; Wang, X.; Guo, T.; Li, P.; Zhao, Y.; Ji, H.; Zhang, L.; Zhou, Z. A peptide mimicking VGLL4 function acts as a YAP antagonist therapy against gastric cancer. *Cancer Cell* **2014**, *25*, 166−180.